Improving aeration systems in saline water: measurement of local bubble size and volumetric mass transfer coefficient of conventional membrane diffusers

J. Behnisch, A. Ganzauge, S. Sander, M. P. Herrling and M. Wagner

ABSTRACT

In this study, for the first time, the influence of the design of conventional membrane diffusers on the volumetric mass transfer coefficient (k_La) and bubble size in tap water (TW) and saline water (SW) was investigated (up to 15 g/L NaCl). By using a new analytical approach, k_La and the bubble size along the ascent of the bubble swarm were measured simultaneously and in real time. The results show that in TW, after collision bubbles merge into larger bubbles by coalescence. In SW, coalescence is inhibited by salt. Due to the smaller bubble size, k_La increases to more than double compared to TW. The results show that in SW, membrane diffusers with dense slit patterns and smaller slit lengths are to be recommended in order to enable improved utilization of oxygen in saline water.

Key words | aeration, bubble size distribution, flexible membrane diffuser, image analysis, oxygen transfer, volumetric mass transfer coefficient

J. Behnisch (corresponding author)
A. Ganzauge
M. P. Herrling
M. Wagner
Technische Universität Darmstadt, Institut IWAR,
Franziska-Braun-Str. 7, 64287 Darmstadt,
Germany
E-mail: *j.behnisch@iwar.tu-darmstadt.de*

S. Sander
WILO GVA GmbH,
Dieselstr. 6, 42489 Wülfrath,
Germany

INTRODUCTION

In biological wastewater treatment plants, nowadays, mainly fine-bubble aeration systems are used to satisfy the oxygen demand of microorganisms in activated sludge. There are different diffuser geometries available (domes, tubes, discs, plates, panels) made out of different materials (ceramic, plastic, flexible membranes) (Burton *et al.* 2014). Oxygen mass transfer from ascending air bubbles to the liquid phase is described by the volumetric mass transfer coefficient (k_La), which represents the product of the liquid-side mass transfer coefficient (k_L) and the liquid/gas interfacial area (a) (Jenkins & Wanner 2014). The k_La mainly depends on water quality parameters (e.g. salt concentration, temperature) and diffuser design. Air bubbles should be as small as possible to maximize a, and thus achieve efficient oxygen mass transfer. The optimum diameter of bubbles in aeration tanks of 4–6 m height is described to be between 0.75 and 1 mm (Motarjemi & Jameson 1978). The bubble size of conventional fine-bubble aeration systems is between 2 and 5 mm and therefore clearly larger than the optimum bubble diameter (Hendricks 2011). In this size range, bubble shape can be approximated by spheres and oblate spheroids (Henkel 2010). It is crucial to include practice conditions when designing diffuser devices. Smaller slit lengths can lead to smaller bubbles, but also to a higher pressure drop across the membrane and increasing the slit density can lead to an insufficient breaking strength of the diffuser membrane (Hasanen *et al.* 2006).

To optimize aeration systems, and in particular gas distribution devices, investigations on bubble size and bubble size distribution (BSD) have therefore already been the subject of studies in past decades. Thereby, digital image analysis has been commonly used as a non-intrusive and cost-effective technique (Busciglio *et al.* 2008). Diverse experiments were conducted in reactors of different sizes and with different diffuser types. Akita & Yoshida (1974) and Botello-Álvarez *et al.* (2011) measured the BSD of bubble swarms generated via porous diffusers. Painmanakul *et al.* (2004) compared two conventional membranes for wastewater aeration. For their tests, they used only one or four holes. Polli *et al.* (2002) utilized perforated diffusers of different design characteristics and measured very large bubbles (4–14 mm on average). Nevertheless, investigations of the BSD of bubble swarms of conventional flexible membrane diffusers are rare. For example, Hasanen *et al.* (2006) determined the BSD in different positions of the bubble swarm (axial and radial) using conventional fine-bubble diffusers in tap water (TW), similar to those used in the present study. They showed that coalescence takes place near the diffuser and appears to depend on the air flow rate. They observed that slit density has a smaller effect on BSD with increasing air flow rates.

doi: 10.2166/wst.2018.358

Highly saline wastewaters occur mainly in coastal regions via the intrusion of seawater into leaky sewers or in case of industrial wastewater. When fine-bubble aeration is applied in wastewater with high salt concentrations, plant operators face the problem of oversized aeration systems. This can be explained cause design approaches of fine bubble aeration systems do not yet take into account the significantly increase of k_La due to the inhibition of bubble coalescence (Sander *et al.* 2017). Firouzi *et al.* (2015) showed that the smaller the bubble diameter, the more salt is needed to inhibit bubble coalescence completely. Therefore, it is obvious that the average bubble size of a bubble column in a coalescence-inhibited system is influenced by salt concentration and diffuser design, due to the different initial bubble diameter. Marrucci & Nicodemo (1967) investigated the influence of different salts on the coalescence behavior in a bubble swarm of porous diffusers. They showed that bubbles detaching from the distributor always have the same size, irrespective of air flow rate and salt concentration. They defined the diameter of the detaching bubbles as *quasi-static bubble diameter*. By increasing the salt concentration, the mean bubble size of the bubble swarm aspired asymptotically to the observed *quasi-static* value. Therefore, they concluded that with diffusers, which produce larger bubbles, coalescence inhibition has a poor effect. However, there is still knowledge missing about the influence of the diffuser design of flexible membrane diffusers on BSD and oxygen transfer at elevated salt concentrations.

The objective of the present study is to combine data of BSD with oxygen transfer tests in TW as well as in saline water (SW), using conventional flexible fine-pore membrane diffusers with different design properties. NaCl was used as one of the most frequent salts in wastewater. Various methods of image analysis were compared to find the best representation of BSD. The influence of slit length and slit density to BSD was investigated with various air flow rates and salt concentrations. The data give new and important indications on the design approaches of membrane diffusers, which are used for aeration of saline wastewater, for optimizing oxygen transfer and energy consumption of aeration systems.

MATERIAL AND METHODS

Membrane diffusers

Two conventional disc diffusers with different slit densities and slit lengths (d_S) were used (Figure 1). Slit density is defined as the number of slits relative to the active (perforated) membrane area. Around a non-perforated center, the slits are arranged in rows with a fixed distance between them (P_r). The distance between the slits of one row (P_s) depends on the slit density.

Oxygen transfer tests

Oxygen transfer tests were performed in a rectangular tank (0.5 m × 0.5 m) with a water depth of 1.0 m (Figure 2), using the pure oxygen desorption method according to ASCE (2007). Several probes (Model 2126, Orbisphere) were installed to record dissolved oxygen concentrations. Finally,

		Diffuser-1	Diffuser-2
Disc diameter	[cm]	26.5	26.5
d_S	[mm]	0.75	1.25
Slit density	[St/cm²]	15.5	10.0
Amount of slits	[-]	5,028	3,063
P_R/d_S	[-]	4.07	2.44
P_S/d_S	[-]	2.15	1.80
Material		EPDM*	EPDM*

* Ethylene-Propylene-Dien-Terpolymere

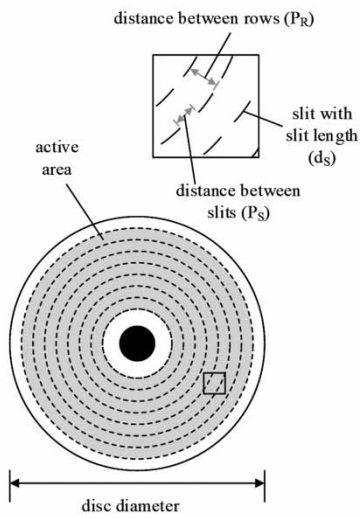

Figure 1 | Properties of the two conventional disc diffusers and a schematic representation.

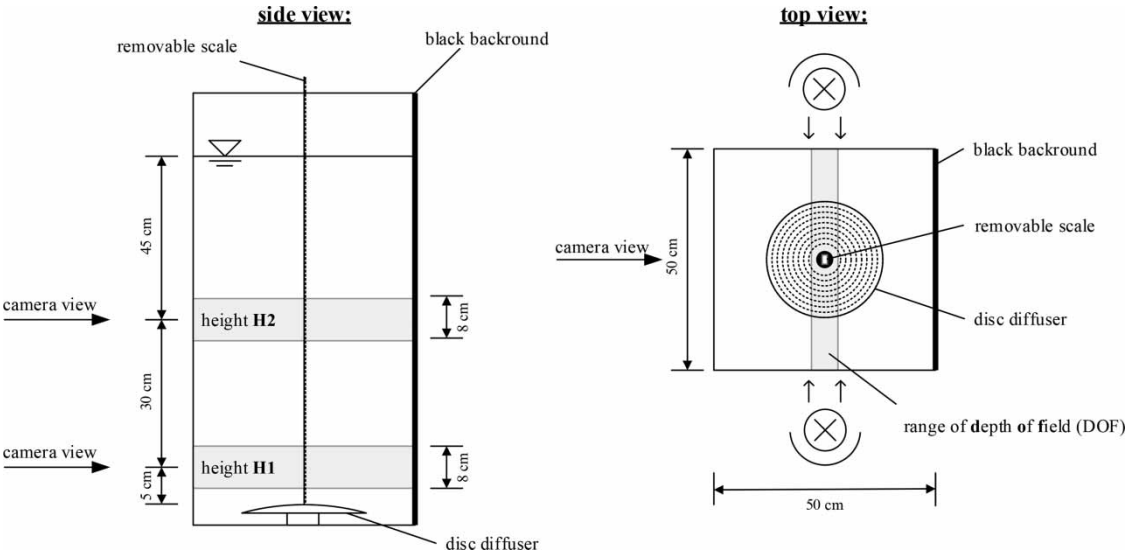

Figure 2 | Reactor made of glass, side and top view.

the k_La for a specific temperature (T) was calculated (k_La_T) by a non-linear regression, which was standardized to 20 °C (k_La_{20}) according to the following equation:

$$k_La_{20} = k_La_T \cdot 1.024^{(20-T)} \quad (1)$$

Tests were performed at different air flow rates (2.0, 3.5 and 4.5 m³/h) and salt concentrations (5, 10 and 15 g/L NaCl). The air flow rate was measured at standard temperature and pressure (STP) with a thermal flow sensor (TA16, Hoentzsch). The first test was carried out in TW; then NaCl was added. The effect of salt on k_La_{20} is described by the f_S-value, which is defined as the ratio between k_La_{20} in SW and in TW (Sander *et al.* 2017):

$$f_S = \frac{k_La_{20,SW}}{k_La_{20,TW}} \quad (2)$$

Bubble size measurement and image analysis

Simultaneously to the measurement of k_La, a digital camera (EOS 70D, Canon) was placed on a tripod in front of the tank for recording images of the bubble swarm in two different heights above the diffuser. Next to the tank two lights for permanent illumination were installed. To best represent the bubble swarm, images were taken at 5 cm (height 'H1') and 35 cm (height 'H2') height above the surface of the diffuser. Before starting aeration, the camera was focused on a scale, which was placed in the center of the tank, in order to evaluate bubble sizes (Figure 3(a)). The camera was set to a low depth of field (DOF) (Figure 2). DOF is the distance between the nearest and farthest object (bubble) giving a focused image (Schröder & Treiber 2007). Bubbles outside DOF are blurred on the images, this way facilitating the identification of overlapping bubbles. For the actual recordings, the settings of the camera (f-number = 4.5; circle of confusion = 0.018 mm; focal length = 50 mm; distance scale to camera = 500 mm; shutter speed = 1/4,000 s; ISO = 5,000) remained constant and yields in a DOF of 15 mm (Schröder & Treiber 2007). The scale was removed and the tests were started.

Image analysis was done with the image processing software ©ImageJ (Rasband, W.S., ImageJ, US National Institutes of Health, Bethesda, ML, USA, https://imagej.nih.gov/ij/, 1997–2016). For each setting, 95–548 bubbles were analyzed. The steps of image processing are depicted in Figure 3(b)–3(f). After binarization and manual thresholding of the original image (Figure 3(b) and 3(c)), single bubbles were defined as regions of interest. Using a macro in ©ImageJ, the bubbles were matched to the best fitting ellipse. False fittings were sorted out manually (Figure 3(d)). As a result of this proceeding, the lengths of the major and the minor axis of the ellipse are given (Figure 3(e)). The geometry of the bubble serves to calculate the bubble diameter (*d*). The three most widely used methods are described here (Figure 3(f)). For method I and method II, a spheroid with the given axis of the ellipse was calculated. For the third dimension, the missing axis was assumed to be equal to the major axis (method I) or the minor axis (method II) (Hasanen *et al.* 2006; Botello-Álvarez

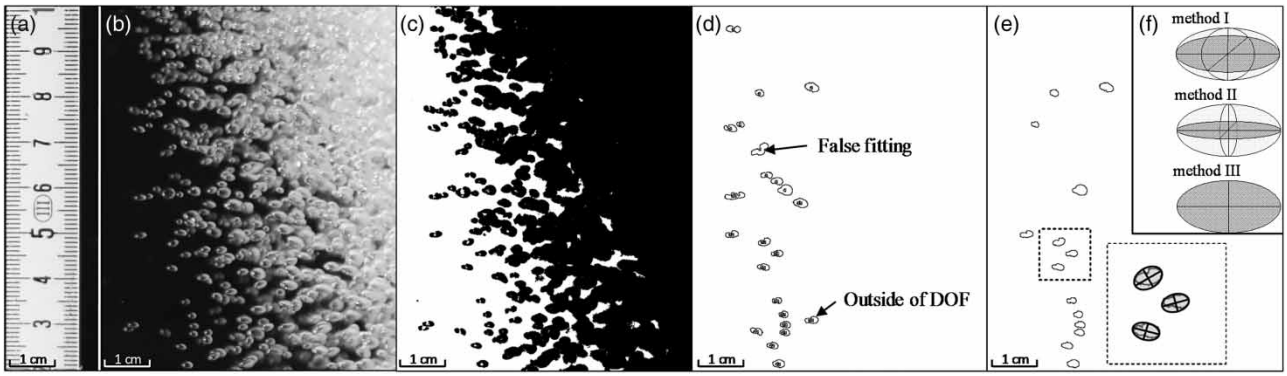

Figure 3 | Image analysis steps: (a) focusing on the scale and measure pixel/distance ratio before starting aeration; (b) original image of the bubble swarm of Diffuser-1 at H1 at 2 m³/h at STP in TW; (c) binarization and thresholding; (d) manual correction of false fitting; (e) major and minor axis of the best fitting ellipse as result; (f) three different methods to calculate the equivalent bubble diameter from 2D images.

et al. 2011). Then, the diameter of a sphere volume-equivalent to the calculated spheroid was defined as the diameter of the bubble. For method III, a circle area-equivalent to the analyzed ellipse was created, its diameter then defined as the diameter of the bubble (Busciglio *et al.* 2008). In this study, all three methods were applied and compared to find the ideal fit of the bubbles. The results of bubble size measurements were grouped into 19 bubble size classes between 0.45 mm and 5.2 mm. To characterize BSD, Sauter mean diameter (d_{32}), relative frequency distribution, skewness (*skew*), standard deviation (σ) and the mean value of the distribution function (d_{mean}) were calculated (Hasanen *et al.* 2006).

RESULTS AND DISCUSSION

Comparison of methods for image analysis

To compare the three presented methods for calculating the equivalent bubble diameter, methods I–III were applied to the same data set. Figure 4(a) shows the calculated equivalent bubble diameter, its frequency, and the corresponding d_{32} value exemplary for one test setting. The courses of the three curves are similar; however, method I shows the highest and method II shows the lowest values in equivalent diameters. The same applies to the calculated d_{32}-values. With respect to d_{32} of method III ($d_{32,\text{method III}}$), d_{32} of method I ($d_{32,\text{method I}}$) and d_{32} of method II ($d_{32,\text{method II}}$) show an average deviation of +11.43% and −9.36%, respectively. Figure 4(b) presents the relative deviation between $d_{32,\text{method I}}$ and $d_{32,\text{method II}}$ to $d_{32,\text{method III}}$ for all test settings for Diffuser-2. No dependency on the test parameters (air flow rate, salt concentration, location above the diffuser) in respect of the deviation of the results between the different methods was observed. This might be due to the uniform bubble shapes during all test settings, i.e. the characteristics of the fitted ellipse (minor-, major-axis, area) always show the same ratio to each other.

The results show that there are large differences between the methods for calculating the equivalent diameter of a three-dimensional bubble from a two-dimensional image. However, the deviation between the results of the three studied methods was systematic. Therefore, while it is not possible to compare specific bubble diameters, it is possible to compare general BSD characteristics from different studies that use different methods of image analysis. To avoid the assumption of the third axis and based on the fact that the absolute bubble diameter is not of interest in the present study, further results are calculated by method III.

Bubble size distribution

Exemplary BSD values for H1 and H2 are shown in Figure 5(a) and 5(b) with the corresponding *skew* and σ values. All distributions are right-skewed (skew >0), i.e. there are predominantly bubbles with $d < d_{mean}$. For Diffuser-1, the distribution in TW for H2 expanded compared with H1 (σ increase, mode class shifts right). This is similar to observations made by Hasanen *et al.* (2006) and Marrucci & Nicodemo (1967). In SW, there was no significant change.

For Diffuser-2, the distribution shows only small changes along the ascent in TW as well as in SW (σ and mode class constant). That leads to the conclusion that the bubble swarm in SW originating from Diffuser-1 is more homogeneous and, in total, consists of smaller bubbles than those originating from Diffuser-2. The BSD from all test settings show the same trends as seen in Figure 5(a)

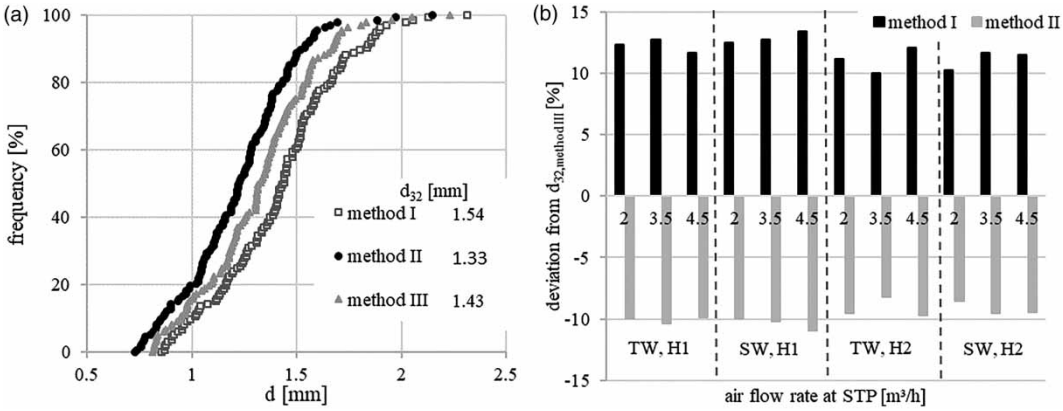

Figure 4 | (a) Histogram of *d* calculated with different methods exemplary for one test setting (Diffuser-1, TW, 2 m³/h at STP, H1); (b) deviation of d_{32} calculated with method I and II in respect to d_{32} calculated with the results of method III for Diffuser-2 on different air flow rates and locations above the diffuser in TW and SW.

and 5(b). The results below will give a deeper insight into this phenomenon.

In order to further characterize the bubble swarm, in Figure 5(c) and 5(d), the d_{32}-values are plotted against the slit-specific air flow rate (dm³/h/St). The results prove that due to the smaller length of slits and the resulting smaller initial bubble size, at H1, bubbles of Diffuser-1 are generally smaller than those of Diffuser-2. The rapid decrease of d_{32} for Diffuser-1 at H2 and 0.9 dm³/h/St at STP (Figure 5(c)) is caused by a faulty measurement: at high air flow rates, there was a strong backflow, which pulled fine bubbles down from the surface of the tank. They were mistakenly

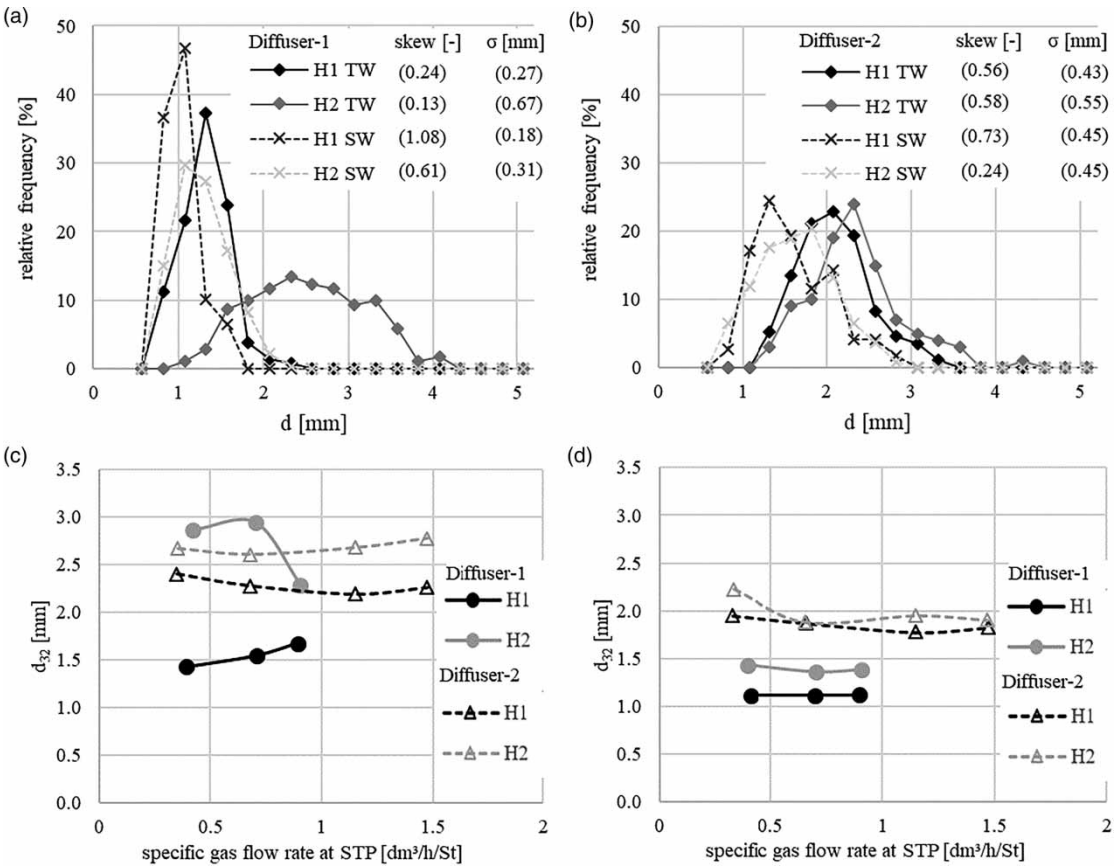

Figure 5 | BSD for Diffuser-1 (a) and Diffuser-2 (b) at 2 m³/h air flow rate at STP in TW and in SW (10 g/L NaCl) and corresponding skew- and σ-values; d_{32} obtained by image analyses for both disc diffusers and different specific air flow rates in TW (c) and SW (d) for H1 and H2.

recorded by image analysis. This problem could be avoided in the case of Diffuser-2 by preventing the backflow during image recording by the installation of a board in the upper part of the tank.

The bubble size in SW at H1 (Figure 5(d)) decreases compared to TW (Figure 5(c)) for both diffusers. This is due to the fact that in TW coalescence takes place along the short ascent between diffuser and H1. Therefore, the bubble size in TW at H1 is larger than the size of the bubbles detaching from the diffuser (=*quasi-static bubble diameter*). In SW, no coalescence occurs even at the ascent between diffuser and H1 and, therefore, the bubble size equals to the *quasi-static bubble diameter*.

In TW, the bubble size of Diffuser-1 increased along the ascent between H1 and H2, while there was no such increase in the bubble size of Diffuser-2 (Figure 5(c)). At H2, the bubble size of both diffusers was in a comparable range. This can be explained by the fact that Diffuser-1 had a higher slit density and, therefore, bubbles are more vulnerable for coalescence (Hasanen *et al.* 2006). At 10 g/L NaCl, coalescence is completely inhibited and the bubble size does not increase along the ascent (Figure 5(d)) and equals to the *quasi-static bubble diameter* also at H2 (Marrucci & Nicodemo 1967). Therefore, bubbles of Diffuser-1 are smaller and provide a larger contact surface for oxygen transfer.

Mostly, bubble sizes increase with rising air flow rates (Marrucci & Nicodemo 1967; McGinnis & Little 2002; Hasanen *et al.* 2006). Orsat *et al.* (1993) showed that for porous materials, the bubble size increases almost linearly with the air flow rate. Some authors described a logarithmical increase (Painmanakul *et al.* 2004). For diffusers with non-uniform pore sizes, Orsat *et al.* (1993) showed that the bubble size decreases with increasing air flow rate until a minimum is reached; then the bubble size increases again. None of the described phenomena was observed in the present study. One possible reason is the relative small range of selected air flow rates. The maximum allowable air flow rate for the used diffusers, as given by the manufacturers (2.6 dm³/h/St at STP for Diffuser-2), could not be reached due to limitations in the test apparatus. Further investigations are therefore necessary.

Oxygen transfer tests

Figure 6(a) shows that the f_S-value for both diffusers increased up to 10 g/L NaCl where it reached its peak value ($f_{S,max}$). Here, bubble coalescence is completely inhibited due to the influence of NaCl. For Diffuser-2, the f_S-value increases with air flow rate. Comparable observations with conventional membrane diffusers in municipal wastewater and TW with sea salt (predominantly NaCl) were described by Sander *et al.* (2017). They describe the dependency between f_S-value and air flow rate by the fact that, at low air flow rates, coalescence also occurs less frequently in TW because of the isolated bubble rise behavior. This is especially relevant in case of lower slit density of Diffuser-2. Here, the bubbles are less vulnerable for coalescence as already discussed before and can be shown in Figure 5(c). Sander *et al.* (2017) also show that at a current salt concentration, the highest f_S-values could be reached at medium air flow rates. Further increasing air flow rate results in a decreasing f_S-value. This effect could not be shown in this work because the necessary high air flow rates could not be reached in the laboratory test tank.

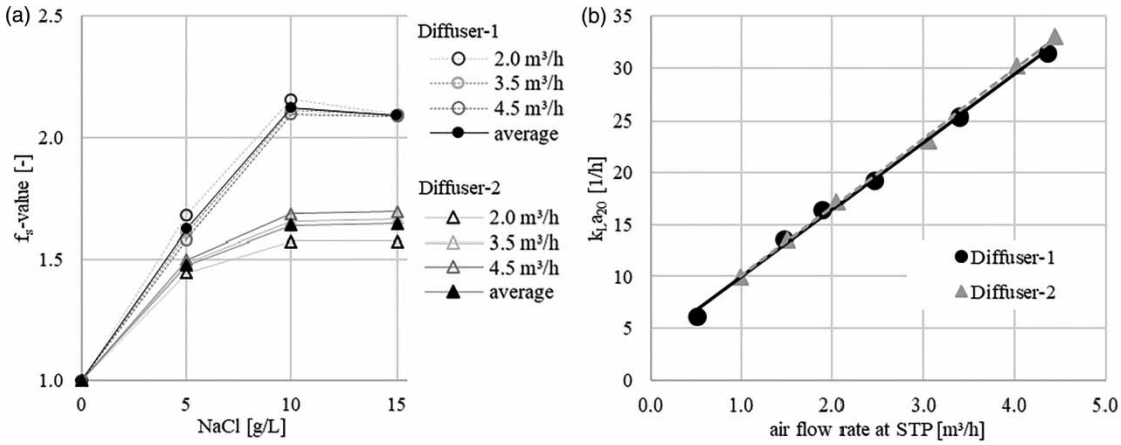

Figure 6 | (a) f_S-values as a function of the salt concentration for both disc diffusers and different air flow rates at STP; (b) k_La_{20} as a function of air flow rate for both disc diffusers in TW.

The present data show that the average $f_{S,max}$ of Diffuser-1 (2.12) is 23% higher than that of Diffuser-2 (1.64). In comparison, k_La-values in TW are in a comparable range for both diffusers (Figure 6(b)). This can be explained by the different bubble sizes produced by the diffusers. With increasing salt concentrations, coalescence is inhibited and the higher slit density of Diffuser-1 in respect of Diffuser-2 has only small impact (Marrucci & Nicodemo 1967). Smaller bubbles generated by Diffuser-1 caused by the smaller slit lengths stay constant along the ascent and offer a larger interfacial area. With the assumption of a homogenous bubble swarm and a typical gas holdup (ϵ) of fine bubble aeration systems of 0.01 (Henkel 2010), in SW, the measured average bubble diameter of 1.25 mm (Diffuser-1) and 1.92 mm (Diffuser-2) and the equation ($a = 6{\cdot}\varepsilon{\cdot}d^{-1}$) from Akita & Yoshida (1974), the interfacial area a can be estimated. According to this simplified calculation, an increase of a in the case of Diffuser-1 (0.048 m²/m³) by 35% in respect to Diffuser-2 (0.031 m²/m³) can be achieved. In comparison, the negative effect of salt on mass transfer coefficient is quite low (Sander *et al.* 2017); consequently, k_La increases.

CONCLUSIONS

The comparison of different methods for image analysis show large differences in the results. The deviation is systematic, thus enabling the comparison of general characteristics of BSD. However, the analytical method has to be taken into account, in case absolute bubble sizes are of interest, e.g. for modelling oxygen transfer.

The combination of oxygen transfer tests and bubble size measurements has shown that membrane diffusers in SW with dense slit patterns and smaller slit lengths are to be recommended. In TW, the use of diffusers with dense slit patterns lead to a rapid increase in bubble size caused by coalescence close to the diffuser. For Diffuser-1, the bubble size increased along the ascent by 93% and reached the same size as the bubbles generated by Diffuser-2. Therefore, in TW, k_La of both diffusers are the same; there was no advantage of the design with dense slit patterns and small slit lengths. In SW, salt inhibits coalescence. Therefore, compared to TW, the bubble size decreases for both diffusers and remains almost constant along the ascent. Nevertheless, bubbles generated by Diffuser-1 (1.25 mm in average) are still smaller than bubbles generated by Diffuser-2 (1.92 mm in average) due to the smaller slit lengths of Diffuser-1. This results in a better oxygen transfer rate due to the higher interfacial area. In SW, k_La of Diffuser-1 increased by 112% compared to TW, while for Diffuser-2, k_La only increased by 64%.

In summary, aeration devices used in SW should be designed with smaller slit lengths and higher slit density in order to generate smaller bubbles. However, there are other parameters than just the bubble size that have to be taken into account in the design (e.g. pressure drop, breaking strength of the membrane), as well. Further research is necessary to define the optimal membrane design for SW application and to investigate the influence of other relevant salts on oxygen transfer rates.

ACKNOWLEDGEMENTS

We thank the German Federal Ministry of Education and Research (BMBF) for funding the research project WaReIp 'Water-Reuse in Industrial parks' (Grant No. 02WAV1409A). We also thank the program committee of the International Young Water Professionals Conferences, organized by IWA, WISA and YWP-ZA, for the support provided by publishing this paper.

REFERENCES

Akita, K. & Yoshida, F. 1974 Bubble size, interfacial area, and liquid-phase mass transfer coefficient in bubble columns. *Industrial & Engineering Chemistry Process Design and Development* **13** (1), 84–91.

ASCE 2007 *Measurement of Oxygen Transfer Rate in Clean Water*. American Society of Civil Engineers, Reston, VA, USA.

Botello-Álvarez, J. E., Baz-Rodríguez, S. A., González-García, R., Estrada-Baltazar, A., Padilla-Medina, J. A., González-Alatorre, G. & Navarrete-Bolanos, J. L. 2011 Effect of electrolytes in aqueous solution on bubble size in gas–liquid bubble columns. *Industrial & Engineering Chemistry Research* **50** (21), 12203–12207.

Burton, F. L., Stensel, H. D. & Tchobanoglous, G. 2014 *Wastewater Engineering: Treatment and Resource Recovery*, 5th edn. McGraw-Hill, New York, NY, USA.

Busciglio, A., Vella, G., Micale, G. & Rizzuti, L. 2008 Analysis of the bubbling behaviour of 2D gas solid fluidized beds: Part I. Digital image analysis technique. *Chemical Engineering Journal* **140** (1), 398–413.

Firouzi, M., Howes, T. & Nguyen, A. V. 2015 A quantitative review of the transition salt concentration for inhibiting bubble coalescence. *Advances in Colloid and Interface Science* **222**, 305–318.

Hasanen, A., Orivuori, P. & Aittamaa, J. 2006 Measurements of local bubble size distribution from various flexible membrane diffusers. *Chemical Engineering and Processing* **45** (4), 291–302.

Hendricks, D. W. 2011 *Fundamentals of Water Treatment Unit Processes. Physical, Chemical, and Biological*, 1st edn. IWA Publishing; CRC Press, London, UK.

Henkel, J. 2010 *Oxygen Transfer Phenomena in Activated Sludge*. PhD thesis, Technische Universität Darmstadt, Germany.

Jenkins, D. & Wanner, J. 2014 *Activated Sludge-100 Years and Counting*, 1 ed. IWA Publishing, London, UK.

Marrucci, G. & Nicodemo, L. 1967 Coalescence of gas bubbles in aqueous solutions of inorganic electrolytes. *Chemical Engineering Science* **22** (9), 1257–1265.

McGinnis, D. F. & Little, J. C. 2002 Predicting diffused-bubble oxygen transfer rate using the discrete-bubble model. *Water Research* **36** (18), 4627–4635.

Motarjemi, M. & Jameson, G. J. 1978 Mass transfer from very small bubbles – The optimum bubble size for aeration. *Chemical Engineering Science* **33** (11), 1415–1423.

Orsat, V., Vigneault, C. & Raghavan, G. S. V. 1993 Air diffusers characterization using a digitized image analysis system. *Applied Engineering in Agriculture* **9** (1), 115–121.

Painmanakul, P., Loubiere, K., Hebrard, G. & Buffière, P. 2004 Study of different membrane spargers used in waste water treatment: characterisation and performance. *Chemical Engineering and Processing* **43** (11), 1347–1359.

Polli, M., Di Stanislao, M., Bagatin, R., Bakr, E. A. & Masi, M. 2002 Bubble size distribution in the sparger region of bubble columns. *Chemical Engineering Science* **57** (1), 197–205.

Sander, S., Behnisch, J. & Wagner, M. 2017 Design of fine-bubble aeration systems for municipal WWTPs with high sea salt concentrations. *Water Science and Technology* **75** (7), 1555–1563.

Schröder, G. & Treiber, H. 2007 *Technical Optics*, 10th edn. Vogel Buchverlag, Würzburg, Germany.

First received 10 April 2018; accepted in revised form 2 August 2018. Available online 14 August 2018